



Publication Year	2017
Acceptance in OA @INAF	2020-09-10T08:37:12Z
Title	Optical, Near-IR, and X-Ray Observations of SN 2015J and Its Host Galaxy
Authors	Nucita, A. A.; De Paolis, F.; Saxton, R.; TESTA, Vincenzo; Strafella, F.; et al.
DOI	10.3847/1538-4357/aa9481
Handle	http://hdl.handle.net/20.500.12386/27273
Journal	THE ASTROPHYSICAL JOURNAL
Number	850

OPTICAL, NEAR-IR AND X-RAY OBSERVATIONS OF SN 2015J AND ITS HOST GALAXY*

A. A. NUCITA,^{1,2} F. DE PAOLIS,^{1,2} R. SAXTON,³ V. TESTA,⁴ F. STRAFELLA,^{1,2} A. READ,⁵ D. LICCHELLI,¹ G. INGROSSO,^{1,2}
F. CONVENGA,¹ AND K. BOUTSIA⁶

¹*Department of Mathematics and Physics “E. De Giorgi”, University of Salento, Via per Arnesano, CP 193, I-73100, Lecce, Italy*

²*INFN, Sez. di Lecce, Via per Arnesano, CP 193, I-73100, Lecce, Italy*

³*European Space Astronomy Centre, SRE-O, P.O. Box 78, 28691, Villanueva de la Cañada (Madrid), Spain*

⁴*INAF, Osservatorio Astronomico di Roma, via Frascati 33, I-00078 Monte Porzio Catone, Italy*

⁵*Department of Physics and Astronomy, Leicester University, Leicester LE1 7RH, U.K.*

⁶*Carnegie Observatories, Las Campanas Observatory, Colina El Pino, Casilla 601, La Serena, Chile*

(Received; Revised; Accepted)

Submitted to ApJ

ABSTRACT

SN 2015J was discovered on April 27th 2015 and is classified as a type II_n supernova. At first, it appeared to be an orphan SN candidate, i.e. without any clear identification of its host galaxy. Here, we present the analysis of the observations carried out by the VLT 8-m class telescope with the FORS2 camera in the R band and the Magellan telescope (6.5 m) equipped with the IMACS Short-Camera (V and I filters) and the FourStar camera (Ks filter). We show that SN 2015J resides in what appears to be a very compact galaxy establishing a relation between the SN event and its natural host. We also present and discuss archival and new X-ray data centred on SN 2015J. At the time of the supernova explosion, Swift/XRT observations were made and a weak X-ray source was detected at the location of SN 2015J. Almost one year later, the same source was unambiguously identified during serendipitous observations by Swift/XRT and XMM-Newton, clearly showing an enhancement of the 0.3-10 keV band flux by a factor ≈ 30 with respect to the initial state. Swift/XRT observations show that the source is still active in the X-rays at a level of ≈ 0.05 counts s⁻¹. The unabsorbed X-ray luminosity derived from the XMM-Newton slew and SWIFT observations, $L_x \approx 5 \times 10^{41}$ erg s⁻¹, places SN 2015J among the brightest young supernovae in X-rays.

Keywords: (stars:) supernovae: individual (SN 2015J)

Corresponding author: A. A. Nucita
nucita@le.infn.it

* Based on observations obtained with XMM-Newton, an ESA science mission with instruments and contributions directly funded by ESA Member States and NASA, with ESO Telescopes at the La Silla-Paranal Observatory under programme ID 298.D-5016(A), and with the 6.5 meter Magellan Telescopes located at Las Campanas Observatory, Chile. We also acknowledge the use of public data from the Swift data archive.

1. INTRODUCTION

It is not obvious that supernova (SN) events may occur in a location of the sky without any associated host galaxy. As a matter of fact, the Sternberg Astronomical Institute (SAI) supernova catalog (Tsvetkov et al. 2004), reports more than 5000 such events whose nature needs to be addressed. In this respect, there is certainly the possibility that the host galaxy is not detected in the majority of the cases because of its low surface brightness or, in a more challenging hypothesis, the SN progenitors are hyper-velocity stars characterized by velocities as large as $\approx 700 - 1000 \text{ km s}^{-1}$ (see e.g. Martin 2006, Brown et al. 2005; Brown 2011; Brown et al. 2014) which have escaped their host galaxy. In both cases, these supernovae are labeled as *orphan SN events*, unless the host galaxy is identified in follow up observations.

SN 2015J is a supernova¹ which occurred on April 27th 2015 at the (J2000) coordinates RA = $07^{\text{h}} : 35^{\text{m}} : 05.18^{\text{s}}$ and DEC = $-69^{\circ} : 07^{\text{m}} : 53.1''$ and observed for the first time by Childress et al. (2015) with the 268-megapixel camera on the SkyMapper 1.3-m telescope at Siding Spring Observatory (Australia) as part of the SkyMapper Transient (SMT) survey (Scalzo et al. 2017). Source images acquired on April 2015 (27.9 UT) had both g and r magnitudes of 19.3.

The SN light curve showed an initial peak of $r = 18.2$ on May (08.9 UT) before declining. The light curve then rose again up to a second peak at $r = 16.8$ on June 09.9 UT. After a brief decline, it rose again and, as noted by the same authors (to whom we refer for more details), the last observation showed a magnitude of $r \approx 16.0$ still rising. Childress et al. (2015) also acquired a 20 minute spectrum with the Wide Field Spectrograph (WiFeS, Dopita et al. 2007) which revealed a Type IIIn SN² located at redshift $z = 0.0054$, correspond-

ing to a distance of $\approx 24.2 \text{ Mpc}$ (adopting the more recent cosmological parameters $H_0 = 67.15 \text{ km s}^{-1} \text{ Mpc}^{-1}$, $\Omega_M = 0.27$ and $\Omega_\Lambda = 0.73$).

The target was also observed with the Australia Telescope Compact Array (ATCA) on June 2015 (29.1 UT) (Ryder et al. 2015) revealing a radio source at a position consistent with that measured optically, and with fluxes of $0.07 \pm 0.02 \text{ mJy}$ and $0.10 \pm 0.03 \text{ mJy}$ at frequencies of 9.0 and 5.5 GHz, respectively.

When searching for an optical counterpart, Childress et al. (2015) found no obvious host galaxy close to the supernovae location and noted that SN 2015J might be associated with a group of galaxies at similar redshifts. In particular, NGC 2434 (at $z=0.004637$ as given by NED) is at a projected distance of 62 kpc and NGC 2442 ($z=0.004890$ via NED) is at 166 kpc. In addition, SN 2015J is close to a $10^9 M_\odot$ gas cloud (HIPASS J0731-69, see Ryder et al. 2001). NGC 2442 seems to interact with HIPASS J0731-69 and the whole complex can be considered as the result of a previous gravitational interaction. However, the two galaxies are too far to explain SN 2015J as originating from a hyper-velocity star progenitor that escaped one of them. It is then natural to expect that the SN occurred in a faint and small galaxy not previously identified.

To address this issue, we obtained ≈ 0.98 hour of net exposure time on the VLT 8-m class telescope with the FORS2 camera in the R filter and a few exposures (180 seconds each) from the Magellan telescope (6.5 m) with the IMACS Short-Camera in the V and I filters and with the FourStar camera in the Ks band. The analysis of these observations, presented in this paper, allowed us to definitely

show signatures of the interaction between the SN ejecta and the circumstellar medium (see, e.g., Schlegel 1990). They form an heterogeneous object sample as their peak luminosity (which span more than two orders of magnitudes, Richardson et al., 2014), depends on many factors such as the circumstellar medium density, the SN ejecta mass and input energy.

¹ The source is also labeled as SMTJ07350518-6907531.

² Type IIIn supernovae are characterized by narrow emission Balmer lines in their spectra (Filippenko 1997) and

show that SN 2015J resides in what appears to be a very compact galaxy, finally establishing a relation between the SN event and its natural host. After comparing the newly acquired data with archival ones (as the Digital Sky Survey -DSS- blue and infrared images³ and the Catalina Sky Survey -CSS-data⁴) we realized that, prior to the SN explosion, the light of the SN progenitor contributed in a non negligible way to the host galaxy brightness (see Section 2 for details).

Type IIIn SN events are among the most luminous X-ray supernovae (see e.g. Chandra et al. 2012 b, 2015), and indeed X-ray observations give important information about the SN itself and its environment. The region of the sky around SN 2015J was observed many times since 2004 by the XMM-Newton satellite in slew mode but without any detection. Also the Chandra observatory did not detect any X-ray source during past observations. At the time of the supernova explosion, Swift/XRT observations were made and a weak source of X-rays was detected at the location of SN 2015J. Almost one year later, the same source was clearly identified during serendipitous observations by Swift/XRT and XMM-Newton, showing an enhancement of the 0.3-10 keV band flux by a factor $\simeq 30$ with respect to the initial state. We requested new Swift/XRT observations which, performed on March and July 2017, clearly show that the source is still active in the X-rays at a level of $\simeq 0.05$ counts s^{-1} , as will be discussed in Section 3.

The paper is organized as follows: in Section 2, we report on archival (DSS and CSS)

³ The Digitized Sky Survey comprises a set of all-sky photographic surveys with the Palomar and UK Schmidt telescopes. The DSS data may be retrieved from <http://archive.eso.org/dss/dss>.

⁴ The CSS, which uses a 1.5 meter telescope on the peak of Mt. Lemmon and a 68 cm telescope near Mt. Bigelow (both in the Tucson area, USA), is a project to discover comets and asteroids and to search for near-Earth objects (NEOs). Further information on the CSS project are available at <http://www.lpl.arizona.edu/css/>.

and newly acquired (VLT/FORS2 and Magellan/IMACS/FourStar) data, while leaving to Section 3 the analysis of all the available X-ray data. We finally present our conclusion in Section 4.

2. SN 2015J: OPTICAL AND NEAR-IR DATA

The absence of a clear identification of the SN 2015J host galaxy makes the event a possible orphan SN candidate. With the aim to find if any extended optical counterpart does exist, we searched for past DSS images acquired in the direction of the target. At the coordinates of the supernova explosion, a source was clearly identified in the DSS survey in the J_{ph} (340 – 590 nm), F_{ph} (590 – 715 nm), and N_{ph} (700 – 970 nm) images. In Figure 1 (left panel), we show the image in the F_{ph} band of the DSS field towards the SN 2015J. The red circle (with radius of $\simeq 1''$) is centred on the nominal coordinates of SN 2015J.

The *Catalogs and Surveys Branch* of the Space Telescope Science Institute digitized the photographic plates from the DSS to produce the Guide Star Catalog which ultimately contains positions, proper motions, classifications, and magnitudes in multiple bands for almost a billion objects down to approximately $J_{ph} = 21$, and $F_{ph} = 20$. The source identified at the SN position has magnitudes in the photographic bands F_{ph} , J_{ph} and N_{ph} of 18.29, 19.61 and 18.26, respectively.

The source identified in the DSS images appears to be point-like and very faint thus opening two possibilities: the DSS source is the unresolved SN 2015J host galaxy or, in the orphan supernovae scenario (Zinn et al. 2012), it is the progenitor of SN 2015J which is believed to be an Eta-Carinae like star (see, e.g. Gal-Yam et al. 2007) which, having an absolute magnitude of $\simeq -12$, at the distance of $\simeq 24.2$ Mpc (as that of the observed supernova), would have a visual magnitude of about 19.5, not far from that corresponding to the DSS source.

To distinguish between these two possibilities, we requested observing time at the VLT telescope equipped with the FORS2 camera in the R filter

(550 nm - 800 nm) and at the Magellan telescope with the IMACS (V and I filters) and FourStar (Ks filter). As far as the VLT/FORS2 data is concerned, each single frame (acquired in December 2016) was corrected using standard procedures (bias, dark current and flat field corrections) and then geometrically aligned in order to get a calibrated and clean image (in counts s^{-1}) as an averaged sum. The VLT/FORS2 R band image resulted in a total exposure time of 0.98 hours. In Figure 1 (right panel), we give a zoom (with histogram equalization) around the target. The green circles (each with a $0.5''$ radius and centred on the centroid of the corresponding brightness surface) on the right panel correspond to some of the sources detected in the the VLT/FORS2 image by using the SExtractor code. We extracted the aperture photometry with a source extraction radius of $\approx 4''$ (i.e. well above the FWHM of the FORS2 camera) while the background was evaluated locally. After calibrating the photometry with the GSC2.3 catalogue (although the photographic band of the DSS plates is similar (but not exactly the same) to the FORS2 R band), the target source resulted to have magnitude (Vega system) in the R band of 18.80 ± 0.20 . The target appeared in the VLT image as a clearly extended source, and we verified its extension by deriving the point spread function (PSF) of the frame by using the DAOPHOT package (Stetson 1987). In particular, we invoked the *find* and *photometry* routines in order to determine the position and aperture photometry of any source above a certain background threshold. We then selected an adequate number of round and isolated (likely PSF) stars. Hence, the DAOPHOT *psf* routine allowed us to estimate an image PSF characterized by a FWHM of $\approx 0.65''$. After subtracting the PSF from the image, we were left with an image of residuals (Figure 2) in which all the star-like objects are removed. Note that large deviations (from what expected for a point-like object) appear at the location of the source and this is con-

vincing evidence we are dealing with an extended object⁵.

As a matter of fact the SExtractor code classified the target as a galaxy (with ellipticity parameter 0.127 and S/G classifier output of 0.03). The extraction radius used in order to encompass the visible halo of the galaxy is $\approx 4''$, corresponding to a linear length of ≈ 0.5 kpc for an estimated distance of 24.2 Mpc as that of SN 2015J.

The distance between SN 2015J and the centroid coordinates of the closest source detected in the FORS2 image is $\approx 0.8''$.

The IMACS and FourStar images were reduced following standard procedures which allowed us to estimate the V, I and Ks magnitude (Vega system) of the host galaxy (possibly with a contribution of the SN, see next discussion) to be 19.68 ± 0.07 , 18.61 ± 0.08 , and 15.80 ± 0.15 , respectively. Note that the photometry of the K band image was obtained by calibrating on the 2MASS catalogue sources found within the field of view, while V and I magnitudes have been calibrated using the standard stars in Landolt field RU149 observed in the same night. As an example, Figure 3 shows a zoom of the field of view around the target as appearing in the FourStar Ks band.

From the discussion above, the presence of the SN host galaxy is evident thus supporting the scenario of SN 2015J being a normal SN occurred in a compact galaxy at a distance of about 24.2 Mpc. As a last remark on the host galaxy, in the NASA's Wide-field Infrared Survey Explorer (WISE, Wright et al. 2010) all sky data, a source was detected in 2010, i.e. well before the supernova explosion. The source had W1 ($3.4 \mu\text{m}$) and W2 ($4.6 \mu\text{m}$) magnitudes of ≈ 15.91 and ≈ 15.89 , respectively.

The multi-band light curve of the target including the CSS data, the data acquired during

⁵ Note that a diffuse brightness surrounds the target and, based on the K image of Figure 3, an emission peak (the *knot* with magnitude 18.77 ± 0.18) is also present in a position located at the South-East from the core.

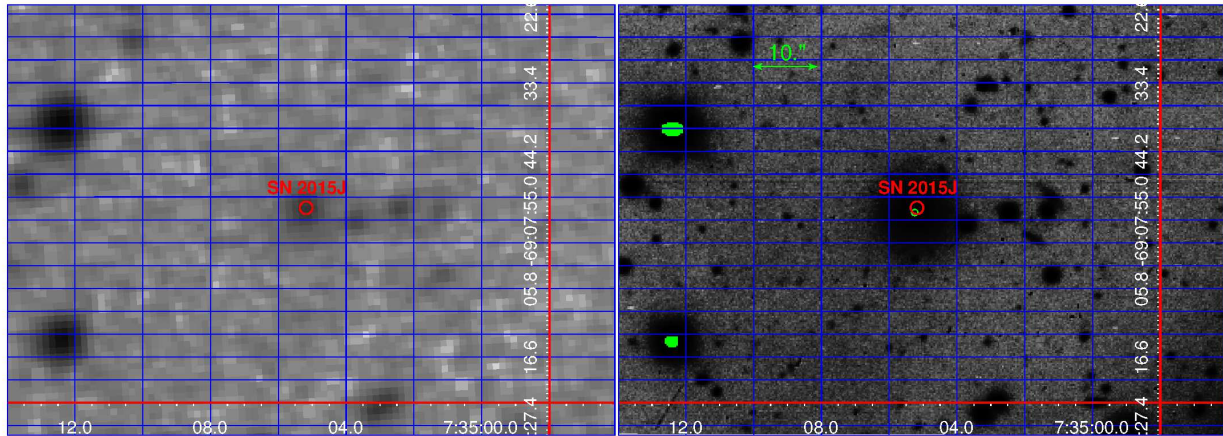


Figure 1. The DSS F_{ph} band image (left panel) and the image acquired by the VLT/FORS2 in R band (right panel) of the region toward SN 2015J are shown. The red circle is centred on SN 2015J. The green circle (with a $0.5''$ radius and centred on the centroid of the corresponding brightness surface) appearing on the right panel corresponds to the source detected in the the VLT/FORS2 image.

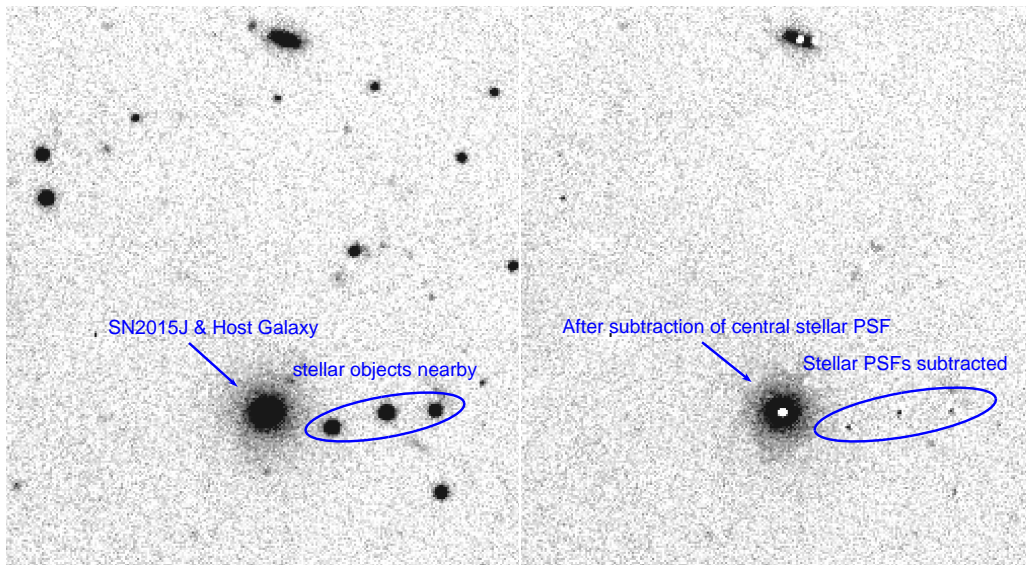


Figure 2. The VLT/FORS2 image of the region around SN 2015J before (left panel) and after (right panel) subtracting the PSF obtained by using DAOPHOT. As it is clear, the target source is an extended object, probably a dwarf galaxy (see text for details).

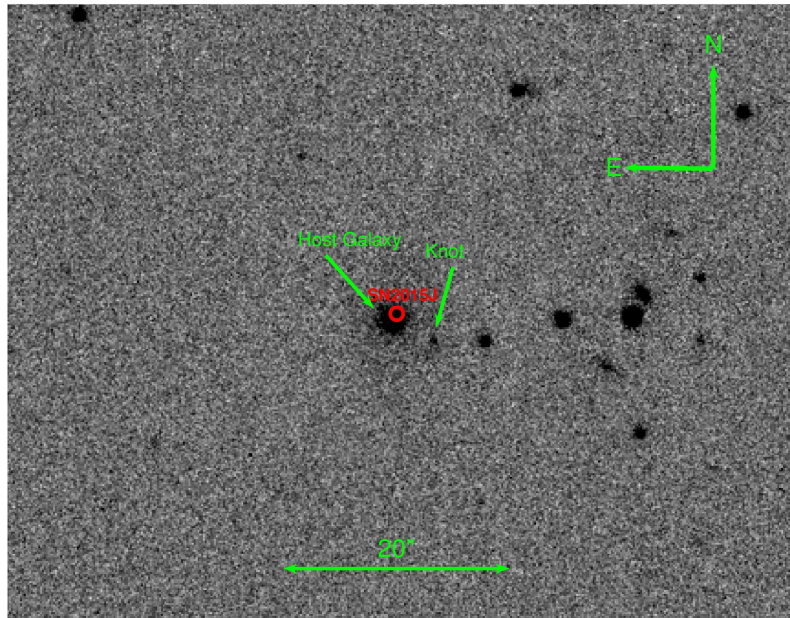


Figure 3. The FourStar Ks image of the galaxy host of SN 2015J.

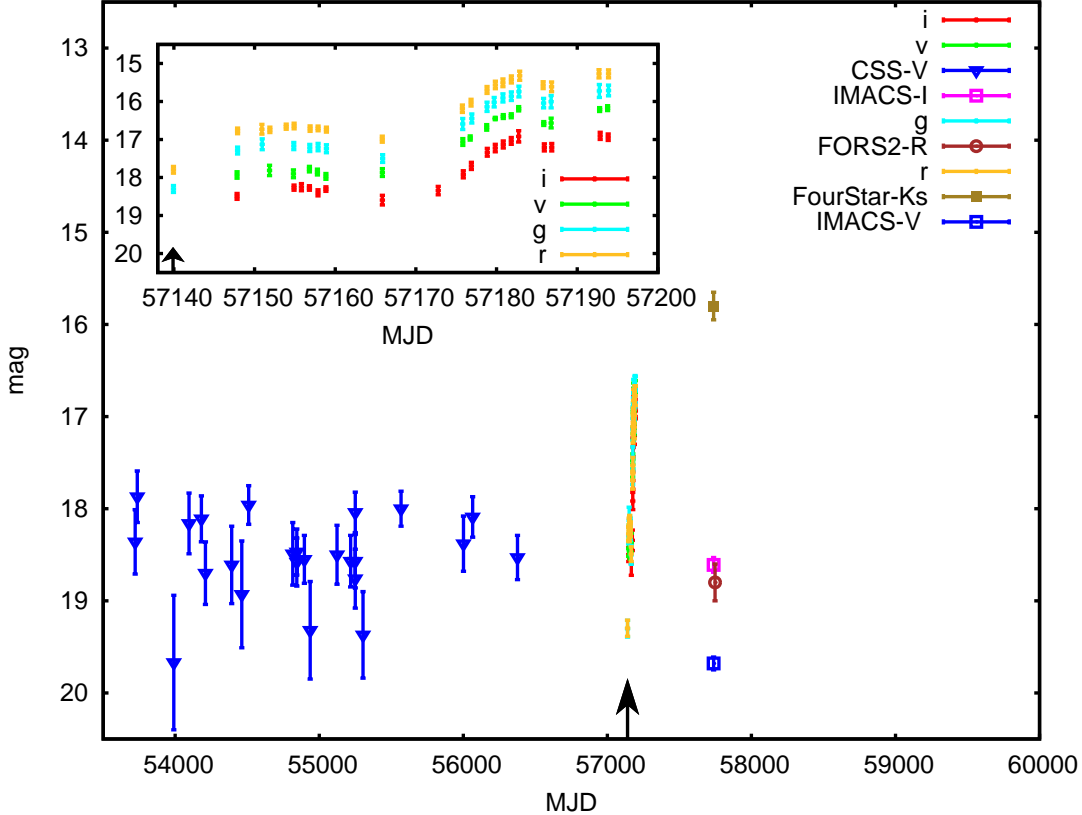


Figure 4. The multi-band light curve of the target including the CSS data (filled triangles, see text for details) is shown. The inset shows a zoom of the light curve (dots as taken directly from [Childress et al. 2015](#)) about the time of the SN event which occurred on April 2015 27.9 UT (corresponding to MJD=57139.9, as also indicated by the black arrow). From *i* to *r* band we applied a recursively offset of 0.5 magnitude for each light curve shown in the inset.

the SN event (as extracted from the figures in [Childress et al. 2015](#)), and the data obtained from VLT and MAGELLAN, is shown in Fig. 4. The inset shows a zoom of the light curve about the time of the SN event with the black arrow indicating the time of the SN explosion. The comparison between the V band magnitude as estimated from the Magellan IMACS data ($\approx 19.68 \pm 0.07$) and the mean value observed in the CSS data before the SN explosion ($\approx 18.52 \pm 0.45$) allow us to conclude that the progenitor of the SN event contributed in a non-negligible way to the host galaxy brightness. In particular, we find $F_{\text{PSN}}/F_{\text{G}} \approx 1.9$, being F_{PSN} and F_{G} the fluxes of the pre SN event and host galaxy, respectively.

3. SN 2015J: THE X-RAY VIEW

The location of SN 2015J was observed in several XMM-Newton slews since 2004 but no source was detected. A Chandra observation (OBSid 2923 antecedent to the SN) did not detect any X-ray source at the position of SN 2015J and put an upper limit to the quiescent X-ray flux of $F_{0.2-8\text{keV}} \approx 6 \times 10^{-15} \text{ erg cm}^{-2} \text{ s}^{-1}$, about 100 times deeper than the XMM-Newton slew upper limits.

SN 2015J was observed by Swift/XRT in several occasions soon after the SN explosion (see Table 1). The Swift data have been analyzed by using the standard procedures described in [Burrows et al. \(2005\)](#) with the latest calibration files. We processed the XRT data with the *XRT-Pipeline* (v.0.12.6) task and we applied standard screening criteria by using the FTOOL (Heasoft v. 6.19). The source spectra have been extracted from a circular region centred on the target nomi-

nal coordinates (with radius of 40 arcseconds) by using the *xselect* routine, while the background spectra were obtained from an annulus with external radius of 60 arcseconds. We then used the *xrtmkarf* script to create the ancillary response files and imported the grouped spectra within *XSPEC* (Arnaud, Dorman, & Gordon 2007) for the spectral analysis.

As shown in Table 1, the Swift/XRT count rate of the target source was $\simeq 7.0 \times 10^{-3}$ counts s^{-1} in the 0.3 – 10 keV energy band during the SN explosion (26th August 2015, 07.46 UT).

The source was serendipitously observed about one year after the SN explosion (in April 2016) by Swift/XRT which detected the source with an increased count rate of $\simeq 5.0 \times 10^{-2}$ counts s^{-1} . On 15th September 2016, observing for 7.2 seconds with the EPIC-pn camera (*XMM*-Newton observation in slew mode, XMMSL1 J073504.6-690752, OBSid 9307100003), a count rate of 1.7 ± 0.4 counts s^{-1} was observed from the source.

Table 1. The log of the Swift/XRT and *XMM*-Newton* (11th row) observations. We give the observation identification number, the (mid) time of exposure, the live time of each observation and the source count rate in the 0.3 – 10 keV band.

OBS ID	T MJD	Live Time s	Rate count s^{-1}
00033857002	57201.532	1743.12	$(2.7 \pm 1.5) \times 10^{-3}$
00033857003	57204.789	1945.40	$(5.3 \pm 1.8) \times 10^{-3}$
00033857004	57207.045	2349.50	$(4.6 \pm 1.6) \times 10^{-3}$
00033857005	57210.735	1860.50	$(4.6 \pm 1.8) \times 10^{-3}$
00033857006	57221.539	1640.72	$(3.6 \pm 1.6) \times 10^{-3}$
00033857008	57236.589	1937.91	$(3.9 \pm 1.7) \times 10^{-3}$
00033857009	57244.098	1997.83	$(5.9 \pm 1.9) \times 10^{-3}$
00033857010	57252.550	1965.38	$(6.7 \pm 2.0) \times 10^{-3}$
00033857011	57260.324	2017.83	$(7.0 \pm 2.0) \times 10^{-3}$
07002410001	57499.501	59.94	$(5.0 \pm 2.9) \times 10^{-2}$
9307100003*	57646.527	7.2	$(9.0 \pm 3.0) \times 10^{-2}$
00033857012	57820.517	1853.00	$(4.9 \pm 0.5) \times 10^{-2}$
00033857013	57946.721	1313.58	$(5.4 \pm 0.6) \times 10^{-2}$

The spectrum was soft⁶, i.e. characterized by an equivalent power-law slope $\Gamma \simeq 3$ or black-body $kT \simeq 0.13$ keV and absorbed flux of $F_{0.3-2\text{keV}} = (2.1^{+1.1}_{-1.0}) \times 10^{-12}$ erg cm^{-2} s^{-1} . The unabsorbed flux, assuming a column density of 2×10^{21} cm^{-2} (Willingale et al. 2013), is $F_{0.3-2\text{keV}} = (7.5^{+3.9}_{-3.5}) \times 10^{-12}$ erg cm^{-2} s^{-1} corresponding to a luminosity of $L_{0.3-2\text{keV}} = (5.2^{+2.7}_{-2.5}) \times 10^{41}$ erg s^{-1} for the esti-

mated distance ($\simeq 24.2$ Mpc) of the host galaxy.

In order to determine the behaviour of the X-ray light curve, we requested new observations of the source by Swift/XRT in March 2017 (Obs ID 00033857012) and again in July 2017 (Obs ID 00033857013) and verified that the source is still active in the X-rays at a level of $\simeq 5.4 \times 10^{-2}$ counts s^{-1} . In Figure 5, we show the 0.3–10 keV light curve in terms of the Swift/XRT PC count rate, where the *XMM*-Newton slew point has been converted to the Swift count rate using the

⁶ Note however that most of the Type IIn supernovae have typically hard X-ray spectra (see, e.g., Chandra et al. 2012 a,b; Stritzinger et al. 2012).

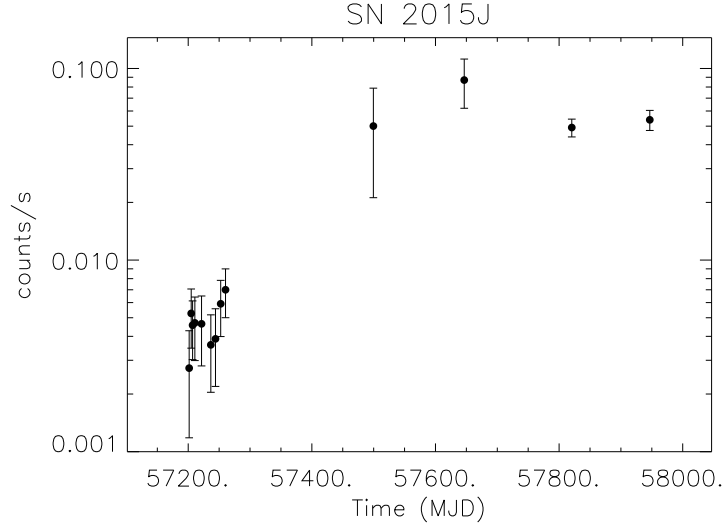


Figure 5. The 0.3 – 10 keV light curve of SN 2015J. The last data point (acquired by SWIFT/XRT in July 2017) shows that the SN event is still active in the X-rays after more than one year at a level of ≈ 0.05 counts s^{-1} . The XMM slew flux at MJD=57646.5 has been converted into a Swift count rate (see text for details).

WebPIMMS tool⁷ and a power-law spectral model (with $\Gamma = 3$). The X-ray flux has been consistently high between August 2016 and the latest observation in July 2017.

A spectrum was extracted from the March 2017 Swift XRT observation and rebinned in order to have at minimum 5 counts per channel with *grp-pha*. The resulting spectrum (presented in Figure 6) appears to be soft. In fact, assuming an absorbed power law with $nH = 2 \times 10^{21}$ cm^{-2} , one gets a power slope of $\Gamma = 4.0 \pm 0.5$ ($\chi^2 = 0.6$ for 15 d.o.f.). The absorbed flux in the 0.3-2 keV band is $(1.1 \pm 0.2) \times 10^{-12}$ ergs cm^{-2} s^{-1} corresponding to an unabsorbed flux of $(6.2 \pm 1.1) \times 10^{-12}$ ergs cm^{-2} s^{-1} . The associated luminosity is $L_{0.3-2keV} = (4.3 \pm 0.8) \times 10^{41}$ erg s^{-1} .

As far as the last Swift XRT observation (July 2017), the spectrum (see Figure 7) can be described by an absorbed power law with $nH = 2 \times 10^{21}$ cm^{-2} and power slope of $\Gamma = 3.5 \pm 0.5$ ($\chi^2 = 0.7$ for 11 d.o.f.). The absorbed flux in the 0.3-2 keV band is $(1.2 \pm 0.3) \times 10^{-12}$ ergs

cm^{-2} s^{-1} corresponding to an unabsorbed flux of $(5.2 \pm 1.3) \times 10^{-12}$ ergs cm^{-2} s^{-1} . The associated luminosity is $L_{0.3-2keV} = (3.6 \pm 0.9) \times 10^{41}$ erg s^{-1} , thus implying an approximately constant X-ray luminosity.

For completeness, the SWIFT/UVOT images (in the U filter centred at 346.5 nm) was analyzed using the *uvotdetect* and *uvotsource* scripts. By performing aperture photometry with a radius of 5'', we found a U magnitude of 19.1 ± 0.1 .

4. RESULTS AND DISCUSSION

We presented the analysis of the observations acquired by the VLT (R band) and Magellan (V, I, and K bands) telescopes as well as the X-ray data from the XMM-Newton (slew mode) and Swift satellites towards the SN 2015J location. Optical and near-IR observations allowed us to discover of the SN host galaxy which appears to be a compact dwarf galaxy with a size of ≈ 1 kpc at a distance of 24.2 Mpc.

The X-ray data show that the SN is still active after about two years after the explosion and the derived unabsorbed X-ray luminosity $L_{0.3-2keV} \approx 5.2 \times 10^{41}$ erg s^{-1} , places SN 2015J among the most luminous young SNe (see Dwarkadas & Gruzsko

⁷ WebPIMMS is available at [urlhttps://heasarc.gsfc.nasa.gov/cgi-bin/Tools/w3pimms/w3pimms.pl](https://heasarc.gsfc.nasa.gov/cgi-bin/Tools/w3pimms/w3pimms.pl)

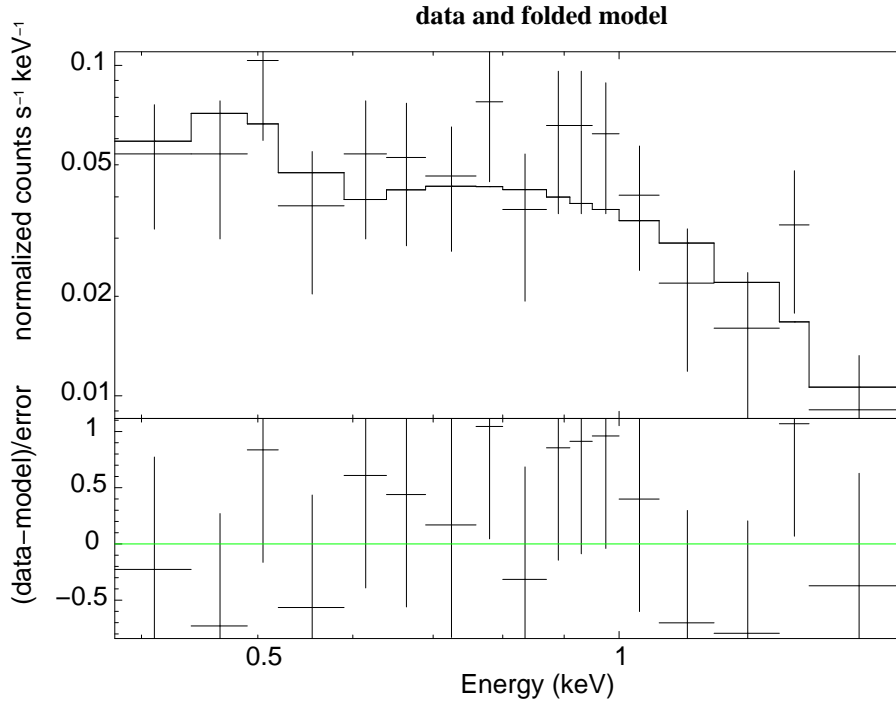


Figure 6. The 0.3-1.7 keV spectrum of SN 2015J as observed by Swift/XRT (OBSid 00033857012).

2012 for a list of SNe observed in X-rays). We note, for comparison, that SN 2010jl was classified as a type IIn supernova with unabsorbed 0.2–10 keV luminosity of about 7×10^{41} erg s^{-1} at 2 and 12 months after the event (Chandra et al. 2012 a). Its spectra could be described by a MEKAL model characterized by a high temperature, $kT > 8$ keV, absorbed by a column which dropped from $nH \approx 10^{24}$ to $nH \approx 3 \times 10^{23}$ cm^{-2} between the observations. Also SN2006jd showed a large X-ray luminosity (about 4×10^{41} erg s^{-1}) for several years after the explosion (Stritzinger et al. 2012). The temperature was also very high here, $kT > 20$ keV with an intrinsic column of $nH \approx 10^{21}$ cm^{-2} (Chandra et al. 2012 b). In these type IIn SNe, the high luminosity has been attributed to a forward shock, from ejecta expanding at several thousands

km s^{-1} into a dense circumstellar medium expelled by the progenitor star in previous shell ejection episodes.

In this respect, we note that SN 2015J has properties in common with these two SNe as regards the optical spectrum and the X-ray luminosity of a few $\times 10^{41}$ ergs/s which persisted for more than a year. However, its X-ray spectrum, as deduced from the admittedly low statistics of the Swift observations, appears to be much softer than the other type IIn SNe. In fact, when fitting the last SWIFT/XRT data (July 2017) with an absorbed MEKAL model (i.e., *wabs*zwabs*mekal* within XSPEC, with the *wabs* component accounting for the galactic hydrogen column density and *zwabs* for any intrinsic absorption) the best-temperature is $kT = 0.17^{+0.4}_{-0.04}$ keV (1σ errors) with an upper limit of ≈ 1.1 keV

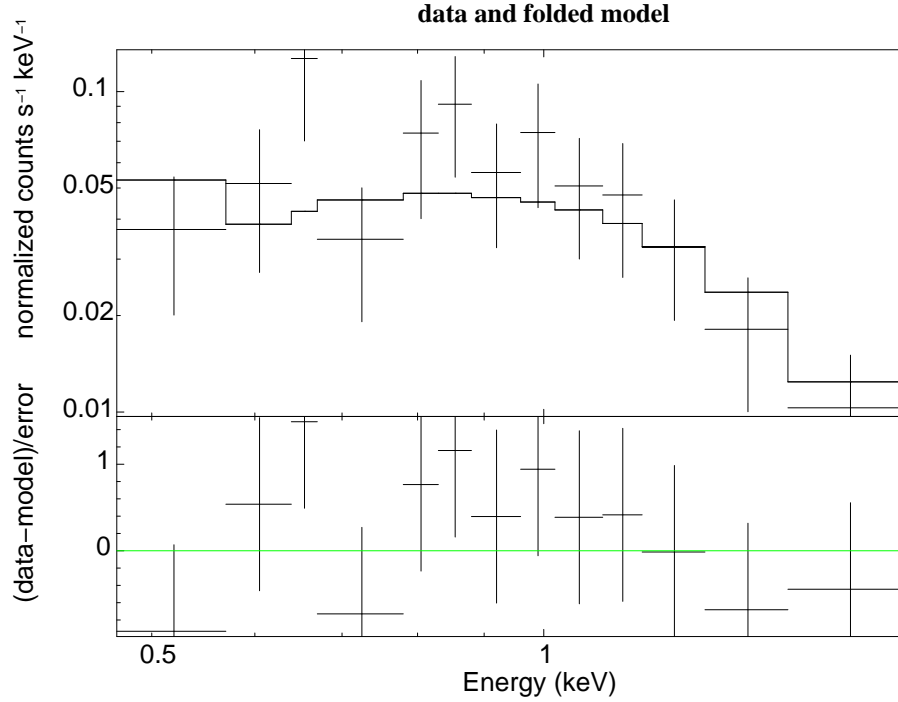


Figure 7. The 0.3-1.7 keV spectrum of SN 2015J as observed by Swift/XRT (OBSid 00033857013).

with a $3-\sigma$ confidence level (see also Fig. 8). Note however that the intrinsic column density remains unconstrained (with maximum allowed value of $\simeq 1.2 \times 10^{22} \text{ cm}^{-2}$).

A detailed discussion about the evolution of the X-ray light curve from young SNe can be found in Dwarkadas et al. (2010) to whom we refer for more details. Here we comment that the expansion of a SN shock wave into the ambient medium produces forward and reverse shocks that heat up the gas to sufficiently large temperatures and produce X-rays. The expected X-ray luminosity is then

$$L_X \sim n_e^2 \Lambda V, \quad (1)$$

where n_e is the electron number density, Λ the cooling function and V the volume of gas involved in the emission. Assuming that the surrounding

medium number density goes as r^{-s} (with $s = 2$ in the case of a steady wind), that the emission originates from a thin shell with size $\Delta r \propto r$ (as in the self-similar case) at distance r from the SN and that $\Lambda \propto r/t$, one gets

$$L_X \sim \frac{r^{4-2s}}{t}. \quad (2)$$

Therefore, the resulting X-ray emission would scale as t^{-1} in the steady wind scenario. Following this discussion, we fitted the last three data points of the 0.3 – 2 keV light curve assuming a model of the form $L_x = at^b$, where a and b are considered free fit parameters. Fitting the log-log data with the previous relation gave a best fit power-law index $b = -0.98 \pm 1.6$. Although, due to the large associated uncertainty, the light curve is consistent with a

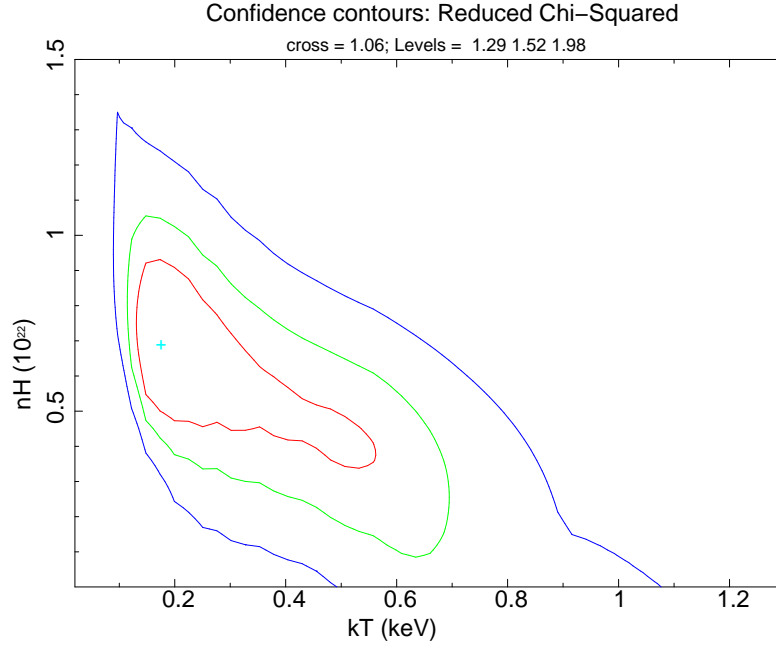


Figure 8. A contour plot of the temperature and absorption column parameters from a fit of an intrinsically-absorbed MEKAL model to the Swift observation of July 2017 (assuming $z = 0.0054$ and galactic column density $nH = 2.0 \times 10^{21} \text{ cm}^{-2}$). Contours mark the 1,2 and 3-sigma errors.

flat slope, the central value of the power-law index seems to be reminiscent of a steady wind whose density decreases as r^{-2} .

However, the column density estimated above is far below the value needed to create the X-ray emission. It is possible that we are observing the shocked emission through a hole in the local gas, as suggested in the case of SN 2006jd by Chandra et al. (2012 b) (see also Katsuda et al. 2016). In addition, the soft spectrum is difficult to be reconciled with the high observed X-ray luminosity if it is generated by shocked material, thus opening to other possible interpretations.

For example, a possibility could be that some part of the material ejected might have remained bound to the compact remnant and fallen back at later times (see, e.g. Dexter & Kasen 2013).

Alternatively, a tidal disruption event might mimic a SN explosion. For example, the superluminous SN event ASASSN-15lh (Dong et al. 2016) has been reinterpreted as the tidal disruption of a star by a rapidly spinning $10^8 M_{\odot}$ black hole by Leoudas et al. (2016) because of the temperature evolution, the total luminosity of the event and the metal-rich host galaxy. Roughly constant, soft ($\Gamma = 3$ or $kT = 0.17 \text{ keV}$), X-ray emission has been seen from the position of ASSASN-15lh with a $L_X \simeq 2 - 8 \times 10^{41} \text{ erg s}^{-1}$ lasting for several hundred days (Margutti et al. 2017).

The power-law index b of the post-peak SN 2015J X-ray light curve is flatter, but still consistent with the canonical TDE decay curve of $t^{-5/3}$, although we note that more slowly evol-

ing TDE light curves are predicted to be common (Guillochon & Ramirez-Ruiz 2013, 2015).

Therefore, future photometric and high precision spectroscopic observations in X-rays are important for addressing the issues that still remain open

on SN 2015J since, if confirmed, it is one of the brightest type II SNe ever observed.

ACKNOWLEDGEMENTS

We acknowledge the support by the INFN projects TAsP (Theoretical Astroparticle Physics Project) and EUCLID. We warmly thank the anonymous Referee for his/her suggestions that improved the paper.

REFERENCES

- Arnaud, K., Dorman, B., Gordon, C., 2007, An X-ray Spectral Fitting Package - User Guide for version 12.4.0, Heasarc Astrophysics Science Division, NASA/GSFC (<http://heasarc.gsfc.nasa.gov/docs/xanadu/xspec/>)
- Brown, W. R., Geller, M. J., Kenyon, S. J., & Kurtz, M. J., 2005, *ApJ*, 622
- Brown, W.R., 2011, *Astronomical Society of the Pacific*, 439, 246
- Brown, W. R., Geller, M. J., & Kenyon, S. J. 2014, *ApJ*, 787, 89
- Burrows, D. N., et al., 2005, *Space Sci. Rev.*, 120, 165
- Chandra, P., Chevalier, R. A., Irwin, C. M. et al., 2012 a, *ApJ*, 750, L2.
- Chandra, P., Chevalier, R.A., Chugai, N., et al., 2012 b, *ApJ*, 755, 110
- Chandra, P., Chevalier, R.A., Chugai, N., Fransson, C., & Soderberg, A.M., 2015, *ApJ*, 810, 32
- Childress, M., et al., 2015, *Atel* #7711.
- Dexter, J., & Kasen, D., 2013, *ApJ*, 772, 30
- Dong, S., et al., 2016, *Science*, 351, 257
- Dopita, M., et al. 2007, *ApSS*, 310, 255
- Dwarkadas, V.V., Dewey, D., Bauer, F., 2010, *MNRAS*, 407, 812
- Dwarkadas, V.V., & Gruszko, J., 2012, *MNRAS*, 419, 1515
- Filippenko, A. V. , 1997, *ARA&A*, 35, 309
- Gal-Yam, A., et al., 2007, *ApJ*, 656, 372
- Guillochon, J. & Ramirez-Ruiz, E., 2013, *ApJ*, 767, 25
- Guillochon, J. & Ramirez-Ruiz, E., 2015, *ApJ*, 798, 64
- Katsuda, S., Maeda, K., Bamba, A., et al., 2016, *ApJ*, 832, 194
- Leloudas, G., et al., *Nature Astronomy*, Volume 1, id. 0002 (2016).
- Margutti et al. 2017, *ApJ*, 836, 25
- Martin, J. C., 2006, *AJ*, 131, 3047
- Richardson, D., Jenkins, R. L., III, Wright, J., & Maddox, L., 2014, *AJ*, 147, 118
- Ryder, S. D., et al., 2001, *ApJ*, 555, 232
- Ryder, S. D., Kool, E., Stockdale, C. J., & Kotak, R., 2015, *Atel* 7762
- Scalzo, R. A., et al., 2017, submitted to *PASA*, arXiv:1702.05585
- Schlegel, E. M., 1990, *MNRAS*, 244, 269
- Stetson, P.B., 1987, *PASP*, 99, 191
- Stritzinger, M., et al., 2012, *ApJ*, 756, 173
- Tsvetkov, D. Y., Pavlyuk, N. N., & Bartunov, O. S., 2004, *Astronomy Letters*, 30, 729
- Willingale, R., Starling, R. L. C., Beardmore, A. P., Tanvir, N. R., & O'Brien, P. T., 2013, *MNRAS*, 431, 394
- Wright, E.L., et al., 2010, *ApJ*, 140, 1868
- Zinn, P.-C., et al., 2012, *A&A*, 538, 30